The (γ,pd) reaction in ^{12}C

S. J. McAllister,* J. C. McGeorge, I. J. D. MacGregor, J. R. M. Annand, S. J. Hall, P. D. Harty,† J. D. Kellie, G. J. Miller,‡ R. O. Owens, D. P. Watts, and T. T-H. Yau§
Department of Physics and Astronomy, University of Glasgow, Glasgow G12 8QQ, Scotland

D. Branford, J. A. MacKenzie,‖ and M. Liang¶
Department of Physics, University of Edinburgh, Edinburgh EH9 3JZ, Scotland

P. Grabmayr, T. Hehl, T. Lamparter,** M. Sauer,†† and R. Schneider††
Physikalisches Institut, Universität Tübingen, D-72076 Tübingen, Germany

J. Ahrens and R. Beck
Institut für Kernphysik, Johannes-Gutenberg Universität, D-6500 Mainz, Germany
(Received 5 May 1999; published 8 September 1999)

The ^{12}C(γ,pd) reaction has been studied for photon energies between 150 and 400 MeV using the Glasgow photon tagging spectrometer and plastic scintillator detectors at the Mainz MAMI electron accelerator. The overall energy resolution was ~6 MeV, sufficient to determine the initial shells of the emitted nucleons. The energy dependence of the cross section and the missing energy and recoil momentum spectra indicate that, for low residual excitation, the reaction proceeds through interaction with the three detected nucleons in a similar manner to the ^{3}He(γ,pd) reaction while the rest of the nucleus acts as a spectator. [S0556-2813(99)00110-7]

PACS number(s): 25.20.Lj, 27.20.+n

I. INTRODUCTION

Although it is only a small part of the total photoabsorption cross section, the (γ,pd) reaction is of interest because it may proceed, at least partly, through mechanisms which directly involve all three emitted nucleons. Extensive study of the ^{3}He(γ,pd) reaction [1–6] has provided data over a wide range of photon energy and emitted-particle angles. Unlike the ^{3}He$(\gamma,pp)n$ [7] and ^{2}H(γ,pn) [8] reactions the ^{3}He(γ,pd) cross section shows no evidence of structure in the $\Delta(1232)$ resonance region. Laget [9] has interpreted this in terms of the effect of isospin selection rules on photon absorption by $T=0$ nucleon pairs. In this treatment two-nucleon diagrams largely account for the observed forward peaking of the proton angular distributions, but these terms alone fail to explain the significant cross section observed at backward proton angles [1] where it is thought that mechanisms involving the participation of three nucleons play an important role [9]. Inclusion of three-nucleon terms raises the calculated cross section above but closer to the experimental data [1,6]. The remaining discrepancy is possibly due to approximations in the calculations such as the absence of the destructive interference amplitude between the three nucleon terms and the (neglected) $T=1$ two nucleon terms [1].

The (γ,pd) reaction has not been studied extensively in nuclei heavier than ^{3}He. Hartmann *et al.* [10] analyzed (γ,pd) events in a study of ^{16}O photodisintegration with 450 MeV bremsstrahlung. They found that the energy dependence of the cross section was very similar to that for the ^{3}He(γ,pd) reaction suggesting a ''quasi-^{3}He'' mechanism where the photon is absorbed on the three detected nucleons while the rest act as a spectator. However, the limited angular coverage of this experiment and inability to determine the residual excitation energy prevented further investigation of this suggestion. It is important to clarify this, because if the (γ,pd) reaction in nuclei is significantly ''^{3}He-like,'' it may yield information on interactions similar to those responsible for three nucleon forces. In the present work measurements of the ^{12}C(γ,pd) reaction were made with tagged photons over a wide range of photon energy and particle angles. The resolution is good enough to determine the shells from which nucleons are emitted, enabling the photon energy and angle dependence of the cross section for ^{12}C(γ,pd) at low missing energy to be compared with those for the ^{3}He(γ,pd) reaction. The observed recoil momentum distributions are compared with the predictions of a simple model which assumes direct interaction with three nucleons in the appropriate shells.

II. EXPERIMENT

The ^{12}C(γ,pd) data presented in this paper were obtained using the Glasgow photon tagging spectrometer [11,12] installed at the 855 MeV Mainz electron microtron MAMI [13]. The collimated tagged photon beam of intensity $\sim 10^8$ s^{-1} was directed on to a graphite target of thickness 0.33 g/cm^2 inclined at 30° to the photon beam. The fraction

*Present address: J. P. Morgan Ltd, London, UK.
†Present address: School of Physics, University of Melbourne, Australia.
‡Present address: Daniel (Europe) Ltd., Larbert, UK.
§Present address: Chase Research, Basingstoke, UK.
‖Present address: Amadeus Data Processing, Munich, Germany.
¶Present address: Thomas Jefferson Lab, Newport News, VA 23606.
**Present address: Nova Data, Karlsruhe, Germany.
††Present address: ZDV, Universität Tübingen, Germany.

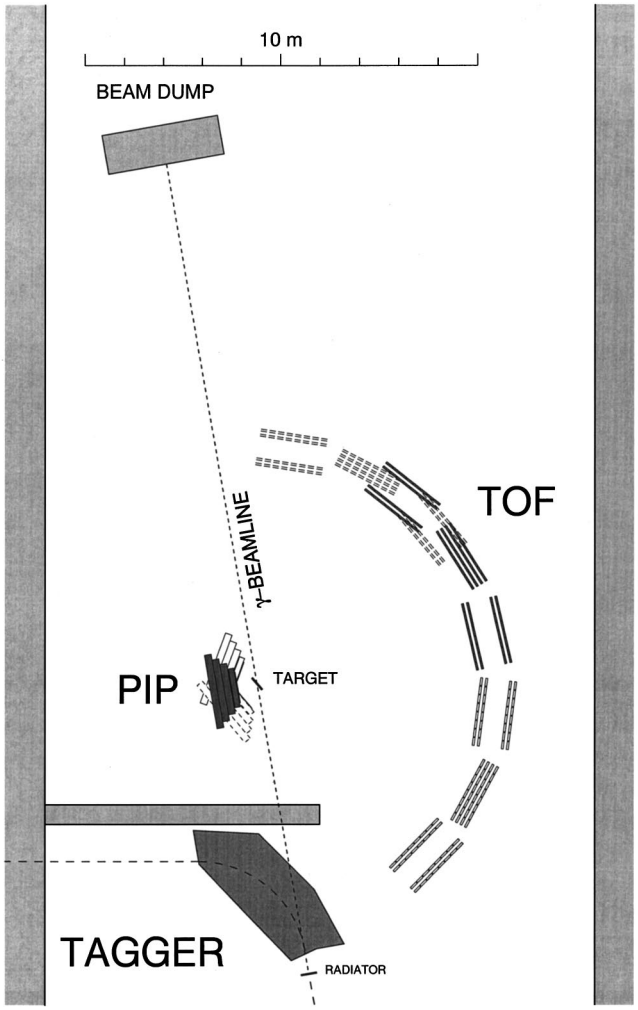

FIG. 1. Schematic of the experimental layout showing the three settings used to detect $^{12}C(\gamma,pd)$ events with forward, central, and backward proton angles.

of photons passing through the collimator (tagging efficiency) was determined by placing a large lead-glass detector directly in the photon beam. The tagging efficiency was found to be stable with an average value of 0.55. The small variation with photon energy is taken into account in the analysis.

Protons were detected in the plastic scintillator hodoscope PiP [14] and deuterons in the time-of-flight array TOF [15]. PiP and TOF cover 0.96 and 0.43 sr, respectively. A 22 cm diameter ring of ΔE detectors made of 1 mm (PiP side) or 2 mm thick plastic scintillator surrounding the target was used to provide a fast trigger and to distinguish charged particles in TOF. Data were taken with the three geometrical settings of PiP and TOF indicated in Fig. 1. The angles covered are listed in Table I, and for each PiP angle TOF largely covers the range that would be necessary for the two-body breakup of ^{3}He. The TOF flight path varied slightly with angle but was $\sim$5.6 m on average. The data were taken in parallel with an experiment on the $^{12}C(\gamma,pn)$ and $^{12}C(\gamma,pp)$ reactions [16] and, to enhance the neutron detection efficiency, TOF was arranged four layers deep. Most of the deuterons are stopped in the first layer.

A coincidence between a signal from appropriate sections of the ΔE ring and at least one element from each of the first two layers of PiP provided the fast trigger for the experiment, but events were rejected unless there were also signals from the TOF array and the tagger focal plane detector array. An additional trigger requirement was that the analogue sum of signals from successive pairs of layers in PiP were above a preset discriminator threshold. This had the effect of a diagonal cut on the successive $\Delta E/E$ two-dimensional displays [14], greatly reducing the number of triggers due to electrons. The main trigger initiated readout of pulse height and time information for all triple hits in PiP, TOF and the tagger. Parallel triggers enabled the readout of cosmic muon events in PiP and events generated by a pulsed light emitting

TABLE I. Summary of angles covered in the forward, central, and backward settings of the proton detector PiP and detector performance over the photon energy range 110–400 MeV.

Detector	Particle	Quantity		Acceptance	Resolution (FWHM)
Tagger	γ	E_γ		110–400 MeV	2 MeV
		E_p		30–330 MeV	4 MeV
			FWD	22.7°–101.1°	
PiP	proton	θ_p	CEN	51.3°–128.6°	3.5°
			BCK	79.0°–156.7°	
		ϕ_p		+22.8°–−22.8°	5.4°
		E_n		$\geqslant$ 17 MeV	5 MeV
		E_d		$\geqslant$ 45 MeV	$\sim$4 MeV
			BCK	10.5°–66.2°	
TOF	neutron/deuteron	$\theta_{n,d}$	CEN	39.6°–95.4°	$\sim$2.0°
			FWD	99.4°–153.4°	
		$\phi_{n,d}$		162.5°–192.7°	$\sim$1°
Combined		E_m	(γ,pn)		7 MeV
		E_m	(γ,pd)		$\sim$6 MeV

diode [17] in TOF, both of which were used to monitor the gain stability.

The requirement of a signal in the ΔE ring which is close to the target greatly reduces the background from the air along the photon beam line. The remaining contribution ($\sim$1.5%) was subtracted using data from runs with the target removed. For detector energy calibration some data were also taken with a 0.22 g/cm^2 perdeuterated polyethylene target.

The hit positions in the PiP and TOF detector elements were determined to within a few cm from the time differences between the signals from the photomultiplier tubes fitted to the two ends of the scintillator bars. Position calibration procedures are described in Ref. [14]. The deuteron polar angles were mainly determined by the location of the TOF elements and the resolution is dominated by the 20 cm element width. For the other particle angles the timing resolution sets the position and therefore the angular resolution. This was measured using the ^{2}H(γ,pn) reaction and the results are given in Table I. Although the value listed for TOF azimuthal angle is for neutrons the resolution for deuterons can be expected to be similar or slightly better because the signals in TOF are, on average, bigger than for neutrons of the same energy. The ^{2}H(γ,pn) reaction was also used to obtain the pulse-height to proton-energy calibration [14] in PiP and to estimate the proton energy resolution (Table I).

The deuteron energies were determined by time-of-flight with suitable corrections for energy losses in the target, ΔE ring and the air along the flight path [18]. The TOF time-to-digital convertors were calibrated using a precision pulser. The ''zero'' times, corresponding to the times of particle emission from the target, were obtained for each TOF element from the sharp peak [15] in the time spectra due to photons produced by atomic scattering in the target. The ^{2}H(γ,pn) data gave a check on the TOF time calibrations and also provided the basis for the estimates of the deuteron energy resolution in TOF and the overall (γ,pd) missing energy resolution listed in Table I. For the first time in a study of the (γ,pd) reaction the resolution is good enough to determine the shells which the nucleons initially occupy, and also allows rejection of most of the events where the energy of the detected particles is reduced by scattering in the final state (FSI).

The pulse-height thresholds for protons in PiP and deuterons in TOF were both less than 10 MeV but, because of energy losses in the target, the ΔE scintillators and the air along the TOF flight path, the effective proton and deuteron energy thresholds are $\sim$30 and $\sim$45 MeV, respectively.

In the data analysis protons in PiP were selected by comparing the total proton energy calculated only from the pulse height in the element in which the particle stops with that calculated from the signals from all PiP layers traversed [14]. In both cases account was taken of the energy losses in wrapping materials, etc., along the particle trajectory. Protons were selected by requiring that the two values agreed to within $\pm$7 MeV. This systematic method excludes almost all of the events where the protons undergo inelastic nuclear collisions in the scintillator, resulting in a false energy signal. Correction for the excluded protons was made by assigning a

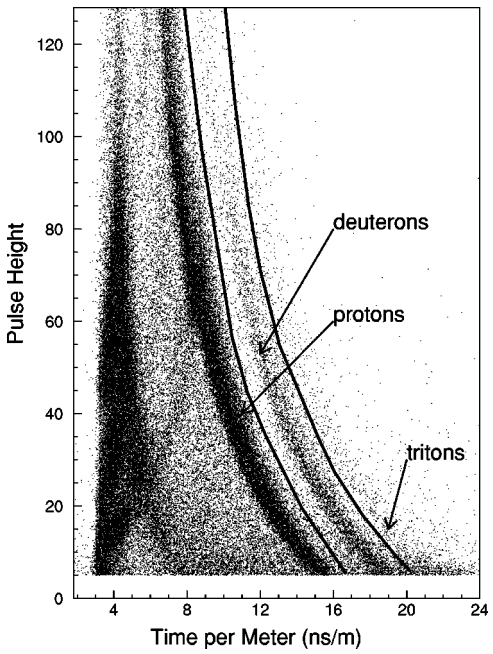

FIG. 2. Two-dimensional plot of pulse height versus inverse speed for charged particles in a TOF detector. The deuteron selection cut is indicated by the solid lines.

weight, which increases with proton energy, to each retained event. These corrections, which are 3.5% at 50 MeV and 26% at 200 MeV, are based on the work of Ref. [19].

Charged particles in TOF were identified by requiring a signal in the appropriate elements of the ΔE ring. Deuterons were selected from plots (Fig. 2) of TOF pulse height versus inverse speed. The possibility that energetic particles, which punch through the front layer, may also suffer significant scattering was accounted for by insisting that a hit in a rear layer came from a charged particle only if energy was also deposited in the TOF element directly in front or in its adjacent neighbors. In that case the time was taken from the front layer, but the pulse heights from both layers were added together giving a better separation of protons from pions. Because the deuteron energies were almost all less than 120 MeV no correction has been applied for inelastic nuclear reactions in the scintillator. Such effects lead to a low energy tail on the pulse height response but, as a result of the rather generous deuteron selection cut, the loss of deuteron yield is less than the tail/total ratio of 1.8% at 50 MeV and 7.5% at 120 MeV estimated from the work of Measday and Schneider [20].

Random coincidences with the tagger were corrected by suitably normalized subtraction of events outside the prompt timing peak in the tagger TDC's. The method of using weights [21] also allowed multiple tagger hits to be properly analyzed. Random coincidences in TOF, estimated from unphysical regions of the particle selection plot, vary from $\sim$2% at forward angles to $\sim$0.5% at backward angles. The cross sections were all reduced by 1.25% to give an approximate correction for this small random contribution.

The results presented in Figs. 3–6 indicate the statistical errors only. It is estimated that systematic errors could be as

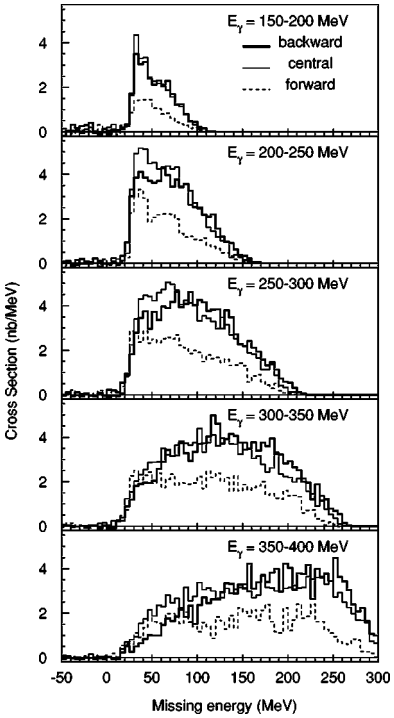

FIG. 3. Missing energy spectra for the ^{12}C(γ,pd) reaction for backward (thick), central (thin), and forward (dashed) proton angles.

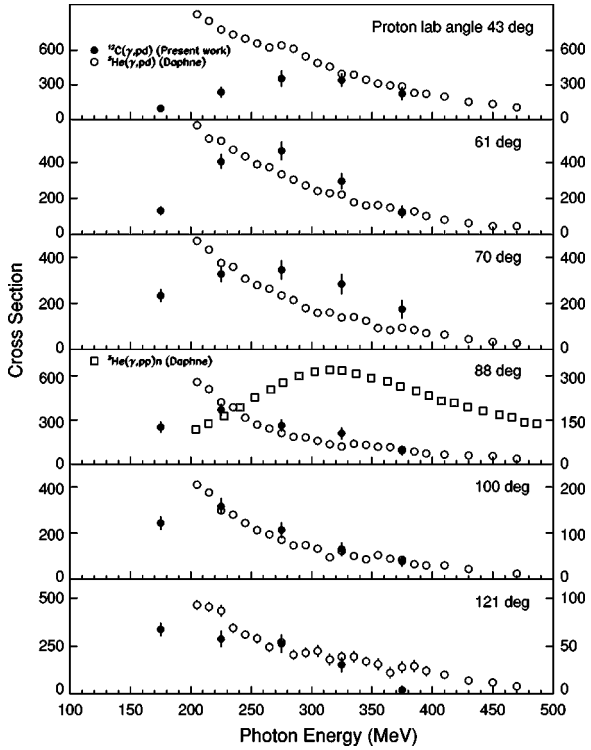

FIG. 4. Photon energy dependence of the ^{12}C(γ,pd) reaction for $E_m<44$ MeV (left scale) compared to that for the ^{3}He(γ,pd) reaction [1] (right scale) and the ^{3}He(γ,pp)n reaction [7] (total cross section, right scale times 50). The ^{12}C data are expressed in units of nb/sr^2, the ^{3}He(γ,pd) data are in nb/sr, and the ^{3}He(γ,pp)n data are in nb.

large as 8%, mostly due to the effects of inelastic nuclear scattering in the scintillators, with smaller contributions from uncertainties in target angle and tagger efficiency.

III. RESULTS AND DISCUSSION

Missing energy and recoil momentum distributions have been valuable in the interpretation [22–24] of (γ,pn) and (γ,pp) reactions. For the (γ,pd) reaction missing energy is defined as $E_m=E_\gamma-T_p-T_d-T_R=S_{pd}+E_x$, where E_γ, T_p, and T_d are, respectively, the energies of the tagged photon and the detected proton and deuteron. T_R is the kinetic energy of the residual system and is derived from E_γ, T_p, T_d and the detected particle angles using conservation of energy and momentum. $S_{pd}=31.7$ MeV is the reaction separation energy and E_x is the excitation of the recoiling system. The missing energy spectra are shown in Fig. 3. At low photon energies there is a peak near threshold and although the strength extends to higher E_m as E_γ increases, it remains significant near threshold especially for forward proton angles. This behavior contrasts with that seen [22–24] in the ^{12}C(γ,pp) reaction where there is no low lying peak, but is more similar to the ^{12}C(γ,pn) reaction. As in that case it suggests that there may be a significant contribution from processes where the photon interacts with and knocks out p-shell nucleons while the rest of the nucleus acts as a spectator. The small bump at $E_m\simeq 50-80$ MeV, most obvious in the forward angle data for 200–250 MeV photon energy, is noticeable in most of the spectra below 300 MeV. It may be due to the involvement of *s*-shell nucleons. There is a shift of relative strength from low to higher E_m as the photon energy and proton angle are increased. This indicates that more than one reaction mechanism contributes and their relative importance changes with photon energy and proton angle.

It is instructive to compare the photon energy dependence of the cross section with that for the ^{3}He(γ,pd) reaction. For this purpose the data were analyzed for 18 deuteron angle ranges, each defined by four TOF detectors as explained in Ref. [16]. For the central angle of each range θ_d an associated proton angle θ_p was calculated from the two-body kinematics of the ^{12}C(γ,pd)^{9}Be$_{\rm g.s.}$ reaction, in which the initial quasi-^{3}He and the residual ^{9}Be nucleus are at rest. The corresponding proton bin was taken as $\theta_p\pm 10°$ to make some allowance for Fermi motion. The emerging particles can suffer an interaction with the residual system, sometimes resulting in extra particles which may or may not be detected. This will usually result in a reduction of the detected particle energy producing an event at high missing energy. As events in the low missing energy region are least likely to be affected by FSI, the comparison is made in Fig. 4 with the present ^{12}C data cut on $E_m<44$ MeV where all three nucleons should come directly from the *p* shell. The ^{12}C(γ,pd) cross sections in Fig. 4 are averages over the proton and deuteron angle bins described above and the ^{3}He data are taken from the measurements made with the DAPHNE detector by Isbert *et al.* [1]. The ^{12}C and ^{3}He data are plotted with different scales to facilitate comparison of the shapes of the photon energy dependence of the cross section. It can be seen that the shapes are similar above $\sim$250 MeV, although

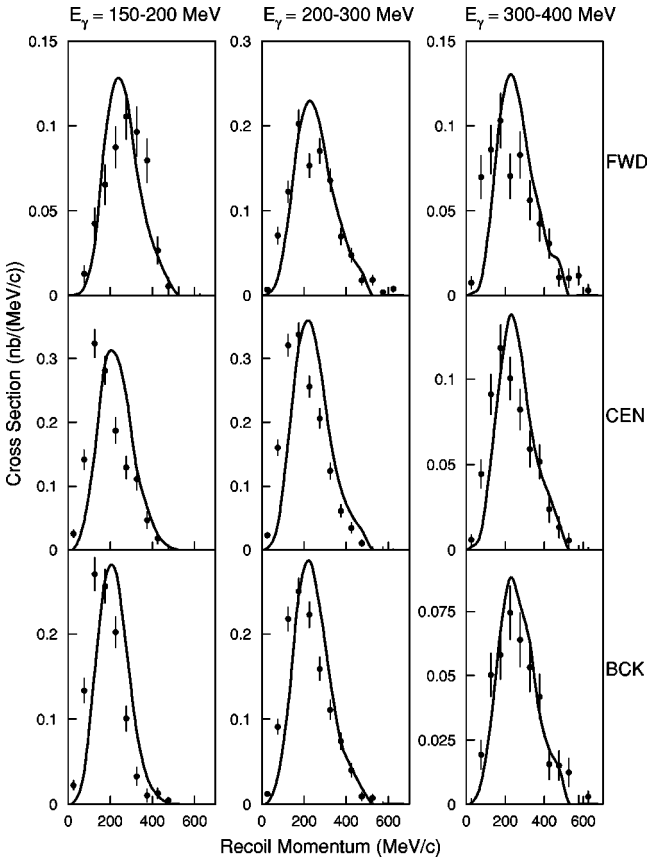

FIG. 5. Recoil momentum distributions for the ^{12}C(γ,pd) reaction for $E_m<44$ MeV. The curves show the distributions predicted by the simple model described in the text. FWD, CEN, and BCK refer to the proton detector angles shown in Fig. 1 and listed in Table I.

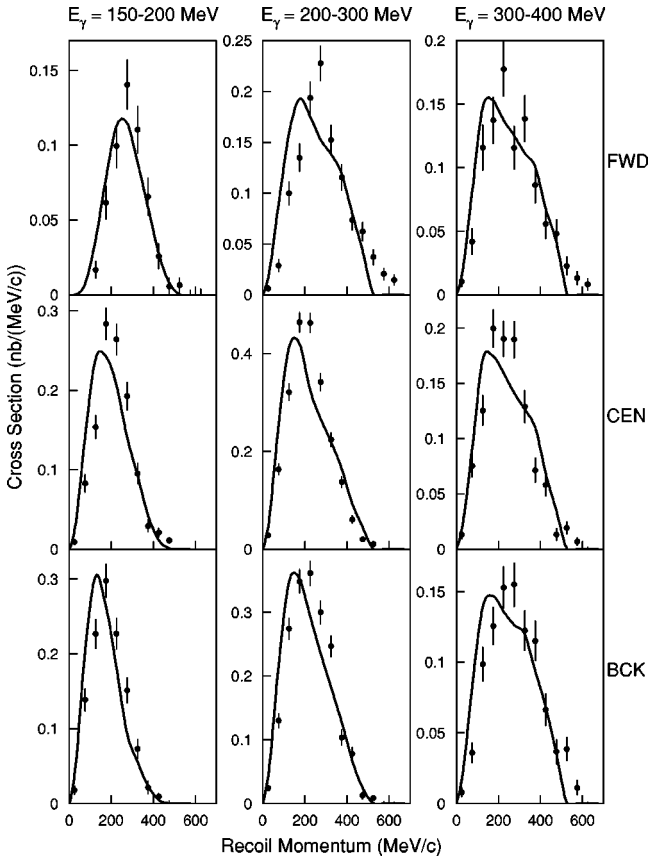

FIG. 6. As Fig. 5 for $E_m=44-70$ MeV.

differences in shape at lower photon energies and forward angles are evident. These are probably due to the effects of the deuteron threshold in TOF, and to Fermi motion which can result in events outside the conjugate angle cuts made in the analysis as described above. Both effects are significant in the present data at low photon energy and forward proton angle. The strong enhancement of the ^{3}He(γ,pp)n cross section found [7] in the region of the $\Delta(1232)$ resonance is not seen in the (γ,pd) reaction either for ^{3}He or ^{12}C. The relative magnitude of the ^{12}C and ^{3}He cross sections suggests that there are few quasi-^{3}He's in ^{12}C, but this may be misleading as many initially produced deuterons probably break up on the way out of the nucleus. Such events could be present in the appreciable high-missing-energy yield seen in ^{12}C(γ,pn) and ^{12}C(γ,pp) reactions [22–24].

The data (for all detection angles) have also been analyzed to obtain distributions of recoil momentum $\mathbf{P}_r=\mathbf{p}_\gamma-\mathbf{p}_p-\mathbf{p}_d$. In a ''three nucleon plus spectator'' model and in the absence of FSI, $\mathbf{P}_r$ is equal in magnitude and opposite in direction to the initial total momentum of the three emitted nucleons. In a simple picture the $\mathbf{P}_r$ distribution can be predicted by folding together [25] three (momentum space) nucleon wave functions. For $E_m<44$ MeV three p-shell wave functions are appropriate while for higher E_m one or more s-shell wave functions is required. In the present work Elton-Swift wave functions [26] were assumed although in the momentum range up to about 250 MeV/c, which is important here, they are very similar to harmonic oscillator wave functions which reproduce the radius of ^{12}C. For this first calculation it was assumed that the three nucleons are at zero separation and therefore are in a relative S state. The effects of detector geometry and thresholds were taken into account by a Monte Carlo procedure similar to that described in Ref. [22].

The model gives a surprisingly good description of the shapes of the $\mathbf{P}_r$ distributions (Figs. 5,6) given that no FSI effects are included. For all photon energies the model predicts less strength at low recoil momentum than is seen in the experiment for $E_m<44$ MeV, while for $E_m=44-70$ MeV it predicts too much strength. Something similar was seen in the ^{12}C(γ,pp) reaction [22,23,27], but in that case it is the higher E_m region in which the ''spectator'' model predicts too much strength. The effect in ^{12}C(γ,pp) has recently been ascribed [27] to the inadequacy of the zero range approximation, used to calculate the initial momentum distribution of the proton pair, which excludes contributions from P (and higher) wave admixtures to the relative wave function of the ''active'' nucleons in the initial state. The addition of such contributions results in terms where the total orbital angular momentum of the $(1p)^2$ pair is $L=1$, in addition to the $L=0,2$ terms allowed for relative S states and greatly improves the agreement with experiment. It is possible that a

similar explanation applies to the $^{12}C(\gamma,pd)$ case, with the reversal of the discrepancy between the two E_m regions due to the parity reversal brought about by the extra *p*-shell nucleon. The assumption that the three active nucleons are in a relative *S* state gives terms with $L=1,3$ for $(1p)^3$ knockout and $L=0,2$ for $(1p)^2(1s)$ knockout. A contribution from nucleons in a relative *P* state would require inclusion of $L=0,2$ terms in the $(1p)^3$ calculation and $L=1,3$ terms in the $(1p)^2(1s)$ case. Because the $L=0$ term provides most of the strength at low recoil momentum the inclusion of *P* waves can be expected to improve the agreement with experiment.

The relative success of the simple model in describing the P_r distributions and the similarity of the photon energy dependence of the cross section to ^{3}He support the idea that in the $^{12}C(\gamma,pd)$ reaction at low missing energy the photon interacts with three nucleons and the residual A-3 nucleus spectates. The lack of strong enhancement of the $^{12}C(\gamma,pd)$ cross section in the $\Delta(1232)$ resonance region is presumably due to the same isospin selection rule effects as in the $^3He(\gamma,pd)$ reaction [9]. Compared to the removal of 3 *s*-shell nucleons from ^{3}He removal of three *p*-shell nucleons from ^{12}C may change the (γ,pd) process in ways other than through the three-nucleon momentum distributions. However the present results suggest that, with development of a proper theoretical treatment, the (γ,pd) reaction at low missing energy may yield information about the correlated behavior of three nucleons in a nucleus.

IV. SUMMARY

This paper presents the first results from measurements on the $^{12}C(\gamma,pd)$ reaction with tagged photons in the energy range 150–400 MeV. The overall resolution of $\sim$6 MeV is good enough to determine the shells from which the emitted nucleons come and to select events which are relatively free of the effects of final state interactions. The E_m spectra show substantial strength at low residual excitation where the cross section shows similar photon energy dependence to that of the $^3He(\gamma,pd)$ reaction. In particular, there is no strong enhancement in the $\Delta(1232)$ resonance region.

The recoil momentum distributions are described surprisingly well by a simple model in which the photon only interacts with the three emitted nucleons while the rest spectate. Further progress will require more sophisticated models which include proper treatment of FSI, as well as experimental investigation in other nuclei.

ACKNOWLEDGMENTS

This work was supported by the U.K. EPSRC, the British Council the DFG (Mu705/3), BMFT (06Tü 656) DAAD (313-ARC-VI-92/118), the EC [SCI.0910.C(JR)], and NATO (CRG 920171, CRG 970268). The authors wish to thank the Institut für Kernphysik der Universität Mainz for the use of its facilities and for its assistance during the experiment. Four of us (J.A.M., S.J.M., D.P.W., and T-Th.Y.) are grateful for support from the EPSRC.

[1] V. Isbert *et al.*, Nucl. Phys. **A578**, 525 (1994).
[2] D. I. Sober, H. Crannell, B. M. K. Nefkens, W. J. Briscoe, D. H. Fitzgerald, R. Goloskie, and W. W. Sapp, Phys. Rev. C **28**, 2234 (1983).
[3] P. E. Argan, G. Audit, N. de Botton, J.-L. Faure, J.-M. Laget, J. Martin, C. G. Schuhl, and G. Tamas, Nucl. Phys. **237**, 447 (1975).
[4] H. J. Gassen, A. Hegerath, W. Loers, B. Mecking, G. Nöldeke, T. Reichelt, and H. Stanek, Z. Phys. **303**, 35 (1981).
[5] P. Picozza, C. Schaerf, R. Scrimaglio, G. Goggi, A. Piazzoli, and D. Scannicchio, Nucl. Phys. **157**, 190 (1970).
[6] N. R. Kolb *et al.*, Phys. Rev. C **49**, 2586 (1993).
[7] G. Audit *et al.*, Nucl. Phys. **A614**, 461 (1997).
[8] R. Crawford *et al.*, Nucl. Phys. **A603**, 303 (1996).
[9] J. M. Laget, Phys. Rev. C **38**, 2993 (1988).
[10] H. Hartmann, H. Hoffman, B. Mecking, and G. Nöldeke, in *Proceedings of the International Conference on Photonuclear Reactions and Applications*, Asilomar, CA, Lawrence Livermore Laboratory Conference No. 730301, 1973 (unpublished), p. 967.
[11] I. Anthony, J. D. Kellie, S. J. Hall, and G. J. Miller, Nucl. Instrum. Methods Phys. Res. A **301**, 230 (1991).
[12] S. J. Hall, G. J. Miller, R. Beck, and P. Jennewein, Nucl. Instrum. Methods Phys. Res. A **368**, 698 (1996).
[13] H. Herminghaus, *Proceedings of the Linear Accelerator Conference*, Albuquerque, NM, 1990 (unpublished); T. Walcher, Prog. Part. Nucl. Phys. **24**, 189 (1990).
[14] I. J. D. MacGregor *et al.*, Nucl. Instrum. Methods Phys. Res. A **382**, 479 (1996).
[15] P. Grabmayr, T. Hehl, A. Stahl, J. R. M. Annand, and R. O. Owens, Nucl. Instrum. Methods Phys. Res. A **402**, 85 (1998).
[16] T. T-H. Yau *et al.*, Eur. Phys. J. A **1**, 241 (1998); I. J. D. MacGregor *et al.*, Phys. Rev. Lett. **80**, 245 (1998); T. T-H. Yau, Ph.D. thesis, University of Glasgow, 1996.
[17] T. Hehl, P. Grabmayr, M. Sauer, and G. J. Wagner, Nucl. Instrum. Methods Phys. Res. A **354**, 505 (1995).
[18] T. Lamparter, Ph.D. thesis, University of Tübingen, 1997; R. Schneider, Ph.D. thesis, University of Tübingen, 1996.
[19] D. F. Measday and C. Richard-Serre, CERN Report No. 69-17, 1969.
[20] D. F. Measday and R. J. Schneider, Nucl. Instrum. Methods Phys. Res. A **42**, 26 (1966).
[21] D. Branford *et al.* (unpublished).
[22] J. C. McGeorge *et al.*, Phys. Rev. C **51**, 1967 (1995).
[23] P. D. Harty *et al.*, Phys. Lett. B **380**, 247 (1996).
[24] T. Lamparter *et al.*, Z. Phys. A **355**, 1 (1996).
[25] S. J. McAllister, Ph.D. thesis, University of Glasgow, 1997.
[26] L. R. B. Elton and A. Swift, Nucl. Phys. **A94**, 52 (1967).
[27] D. P. Watts *et al.* (unpublished).